COMMUNICATION CONSTRAINTS AND ASYNCHRONOUS MEASUREMENTS IN DECENTRALIZED KALMAN FILTERS

M.S. Schlosser and K. Kroschel

Institut für Nachrichtentechnik
Universität Karlsruhe
76128 Karlsruhe, GERMANY
{schlosser, kroschel}@int.uni-karlsruhe.de

ABSTRACT

Decentralized Kalman Filters are often used in multi-sensor target tracking as such a distributed fusion architecture has several advantages compared with centralized ones. On the other hand, distributed fusion is not only conceptually more complex but the required bandwidth is also likely to be a lot higher. However, a trade-off between bandwidth and performance is possible. In this work, the quantitative amount of performance degradation due to infrequent communication between the fusion nodes is investigated in a typical tracking scenario. Furthermore, as a conclusion, a simple approach to deal with asynchronous measurements is proposed.

1. INTRODUCTION

In target tracking, multi-sensor systems are becoming more and more popular. The advantages especially for physically distributed sensors are obvious: multiple viewing angles, different strong points of different sensors and higher robustness due to the inherent redundancy. On the other hand, some kind of fusion is necessary to integrate the data from the different sensors and to extract the desired information about the targets.

Traditionally, a centralized fusion architecture was used, where all the data from the different sensors was sent to a single location to be fused. In recent years, increasing emphasis has been placed on distributed fusion where several fusion nodes exist in the network, like e.g. the Decentralized Kalman Filter (DKF). The advantages of such a distributed fusion architecture are: lower processing load at each fusion node, higher robustness due to redundancy of fusion nodes and easier detectability of malfunctioning sensors.

On the other hand, distributed fusion is not only conceptually more complex but the required bandwidth is also likely to be a lot higher compared with centralized fusion. This is especially true if the final estimate shall be obtained at several fusion nodes. However, a trade-off between bandwidth and performance is possible by letting the fusion nodes communicate at reduced rates.

Most research on DKFs assumed unlimited communication bandwidth between the different processing nodes [1, 2]. In [3] and [4], it was already pointed out that the information of the different local processors becomes correlated due to propagating the same underlying process noise if the communication rate is reduced. However, no quantitative measures for the amount of performance degradation were given. This shall be investigated here.

Sensors running at different observation rates are an important issue in distributed target tracking, too. In [5], a rather complex algorithm was deduced to cope with asynchronous measurements in a DKF requiring feedback from the FC to the LKFs. Based on our findings concerning the reduction in communication rate, a simple alternative to treat asynchronous measurements will be presented here.

To keep the treatment simple, we want to focus on communication issues in a simple DKF consisting of two Local Kalman Filters (LKFs) producing track estimates based on a single local sensor and a Fusion Center (FC) combining these local estimates to a global one.

2. DECENTRALIZED KALMAN FILTER

For a Kalman Filter (KF) to be applicable, the target's dynamics need to be modeled by the following state space equation

$$\mathbf{x}(k+1) = \mathbf{F}\mathbf{x}(k) + \mathbf{w}(k)\,, \tag{1}$$

where $\mathbf{x}(k)$ is the state vector of the target at time instant k, $\mathbf{F}$ is the time-invariant state transition matrix and $\mathbf{w}(k)$ a white noise sequence with covariance matrix $\mathbf{Q}(k)$ representing the process noise.

Respectively, the linear measurement models are given by

$$\mathbf{y}_i(k) = \mathbf{H}_i\mathbf{x}(k) + \mathbf{v}_i(k)\,, \tag{2}$$

where $\mathbf{y}_i(k)$ is the observation vector containing the position measurement of the i^{th} sensor, $i = 1,\ldots,N$, $\mathbf{H}_i$ is the corresponding measurement matrix and $\mathbf{v}_i(k)$ a zero-mean, white noise sequence with covariance matrix $\mathbf{R}_i(k)$ representing the measurement noise.

The LKFs produce estimates $\hat{\mathbf{x}}_i(k|k)$ based on the information available from a single sensor i using the standard KF equations (see e.g. [6]). At the FC, these estimates are fused together to form the overall state estimate $\hat{\mathbf{x}}_{\text{DKF}}(k|k)$ [3]

$$\begin{aligned}\mathbf{P}^{-1}_{\text{DKF}}(k|k) &= \mathbf{P}^{-1}_{\text{DKF}}(k|k-1) \\ &\quad + \sum_{i=1}^{N}\left[\mathbf{P}_i^{-1}(k|k) - \mathbf{P}_i^{-1}(k|k-1)\right] \qquad (3)\\ \hat{\mathbf{x}}_{\text{DKF}}(k|k) &= \mathbf{P}_{\text{DKF}}(k|k)\Big(\mathbf{P}^{-1}_{\text{DKF}}(k|k-1)\hat{\mathbf{x}}_{\text{DKF}}(k|k-1) \\ &\quad + \sum_{i=1}^{N}\left[\mathbf{P}_i^{-1}(k|k)\hat{\mathbf{x}}_i(k|k)\right. \\ &\quad \left. - \mathbf{P}_i^{-1}(k|k-1)\hat{\mathbf{x}}_i(k|k-1)\right]\Big)\,, \qquad (4)\end{aligned}$$

This work is part of the Sonderforschungsbereich (SFB) No. 588 *"Humanoide Roboter - Lernende und kooperierende multimodale Roboter"* at the University of Karlsruhe. The SFB is supported by the Deutsche Forschungsgemeinschaft (DFG).

where $\mathbf{P}_{\text{DKF}}$ and $\mathbf{P}_i$ are the error covariance matrices of the state estimates $\hat{\mathbf{x}}_{\text{DKF}}$ at the FC and $\hat{\mathbf{x}}_i$ at the LKFs, respectively.

This state estimate is equivalent to the one in the centralized KF as the measurement $\mathbf{y}_i(k)$ weighted with its inverse covariance matrix is equivalent to the gain in information between the predicted local estimate $\hat{\mathbf{x}}_i(k|k-1)$ and the corrected one $\hat{\mathbf{x}}_i(k|k)$:

$$\mathbf{H}_i^T \mathbf{R}_i^{-1}(k)\mathbf{y}_i(k) = \mathbf{P}_i^{-1}(k|k)\hat{\mathbf{x}}_i(k|k) - \mathbf{P}_i^{-1}(k|k-1)\hat{\mathbf{x}}_i(k|k-1). \quad (5)$$

Equations (3) and (4) of the DKF require the LKFs to communicate their corrected local estimates $\hat{\mathbf{x}}_i(k|k)$ along with the inverses of the corresponding error covariance matrices $\mathbf{P}_i^{-1}(k|k)$ to the FC after each measurement. The predicted estimates $\hat{\mathbf{x}}_i(k|k-1)$ and inverse covariance matrices $\mathbf{P}_i^{-1}(k|k-1)$ can either be transmitted as well or calculated at the FC to save half of the bandwidth. Nevertheless, this typically requires more bandwidth than merely communicating the current measurement $\mathbf{y}_i(k)$ along with its error covariance matrix $\mathbf{R}_i(k)$, as required by the centralized KF. These are normally of a lower dimension.

To save even more bandwidth, it is also possible to give up optimality and to let the LKFs communicate with the FC less frequently. Therefore, all predictions by one step need to be replaced with predictions by m steps in (3) and (4), where $m > 1$ is the factor by which the update rate at the FC is reduced. The thus obtained estimates will be denoted $\mathbf{P}_{\text{DKFm}}^{-1}(k|k)$ and $\hat{\mathbf{x}}_{\text{DKFm}}(k|k)$ in the sequel.

On the other hand, the update rate and thus the performance of the LKFs is not affected. The LKFs still run at the sensor observation rate. For dynamic states with process noise, the performance of this fusion process only degrades as the information provided by the different sensors becomes correlated due to propagating the same underlying process noise [3, 4].

For less and less frequent communication between the LKFs and the FC, i.e. $m \to \infty$, the information contained in the predicted state estimates becomes less and less reliable. This is represented by the inverses of the corresponding error covariance matrices approaching zero. Thus, no weight is given to these estimates and they can be discarded in (3) and (4) leading to

$$\mathbf{P}_{\text{simple}}^{-1}(k|k) = \sum_{i=1}^{N} \mathbf{P}_i^{-1}(k|k) \quad (6)$$

$$\hat{\mathbf{x}}_{\text{simple}}(k|k) = \mathbf{P}_{\text{simple}}(k|k) \sum_{i=1}^{N} \mathbf{P}_i^{-1}(k|k)\hat{\mathbf{x}}_i(k|k). \quad (7)$$

This is equivalent to assuming that the local state estimates $\hat{\mathbf{x}}_i(k|k)$ and $\hat{\mathbf{x}}_j(k|k)$ are uncorrelated for all $i \neq j$. Therefore, the estimate $\hat{\mathbf{x}}_{\text{simple}}(k|k)$ can serve as a worst case scenario. More frequent communication necessarily leads to better estimates. Furthermore, $\hat{\mathbf{x}}_{\text{simple}}(k|k)$ can be calculated for every time instant k and not only every m^{th} one as would be the case for $\hat{\mathbf{x}}_{\text{DKFm}}(k|k)$. Thus, less simulation time is needed to achieve statistically significant results.

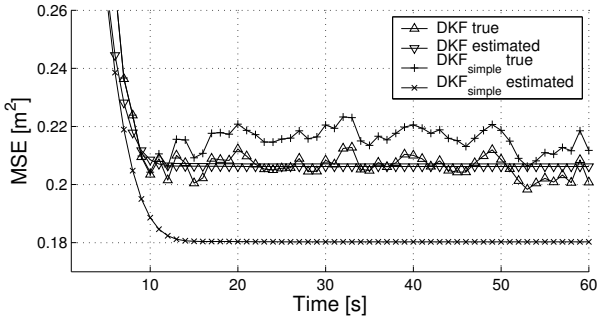

Figure 1: Comparison between true and estimated MSE of DKF and $\text{DKF}_{\text{simple}}$ ($N_0 = 0.01\,\frac{\text{m}^2}{\text{s}^4\text{Hz}}$, $T_s = 1\,\text{s}$, $\sigma_{v,1} = \sigma_{v,2} = 1\,\text{m}$)

3. SIMULATION RESULTS

To obtain quantitative measures of the performance degradation due to infrequent communication, simulations about a target moving at constant velocity tracked by two sensors in the 1D case, as described by the following model, have been performed

$$\begin{bmatrix} x(k+1) \\ \dot{x}(k+1) \end{bmatrix} = \begin{bmatrix} 1 & T_s \\ 0 & 1 \end{bmatrix} \begin{bmatrix} x(k) \\ \dot{x}(k) \end{bmatrix} + \mathbf{w}(k) \quad (8)$$

$$y_i(k) = \begin{bmatrix} 1 & 0 \end{bmatrix} \begin{bmatrix} x(k) \\ \dot{x}(k) \end{bmatrix} + v_i(k), \quad i = 1,2, \quad (9)$$

where

$$\mathbf{w}(k) = \int_0^{T_s} \begin{bmatrix} T_s - t \\ 1 \end{bmatrix} u(kT_s + t)\,dt \quad (10)$$

i.e. the target follows a constant velocity model that is excited by zero-mean continuous random noise $u(t)$ with power spectral density N_0, leading to the following process noise covariance matrix

$$\mathbf{Q} = \begin{bmatrix} \frac{1}{3}T_s^3 & \frac{1}{2}T_s^2 \\ \frac{1}{2}T_s^2 & T_s \end{bmatrix} N_0. \quad (11)$$

Both sensors can only measure the position of the target with variances $\sigma_{v,i}^2$. T_s denotes the sampling rate. There was no mismatch between the model generating the trajectory of the target and the model assumed by the DKF.

Fig. 1 presents the comparison between the true and estimated MSE of the position component in $\hat{\mathbf{x}}_{\text{DKF}}(k|k)$ (4) and $\hat{\mathbf{x}}_{\text{simple}}(k|k)$ (7) for a typical example where $N_0 = 0.01\,\frac{\text{m}^2}{\text{s}^4\text{Hz}}$, $T_s = 1\,\text{s}$ and $\sigma_{v,1} = \sigma_{v,2} = 1\,\text{m}$. $\sigma_{v,1} = \sigma_{v,2}$ ensures that both sensors have the same impact on the final estimate, which presents the worst case. The "true" MSEs were thereby averaged on 5000 Monte Carlo runs.

It can be seen how the DKF slightly outperforms the $\text{DKF}_{\text{simple}}$. Furthermore, the DKF estimates its accuracy correctly whereas the $\text{DKF}_{\text{simple}}$, although performing slightly worse, estimates its accuracy even higher than the one of the DKF. These two phenomena will be studied in detail in the followings.

Fig. 2 displays the true MSEs of DKF and $\text{DKF}_{\text{simple}}$ averaged over time as a function of the spectral density of the process noise N_0. The measurement noises were again set to

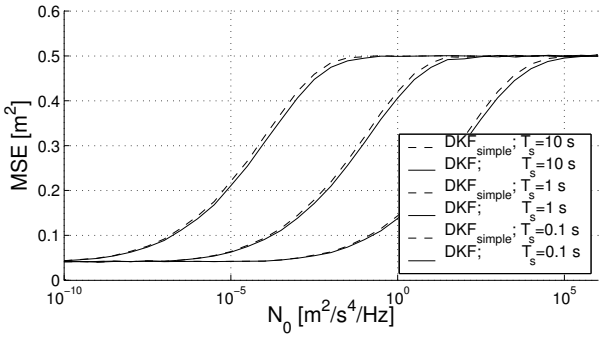

Figure 2: Comparison between $\mathrm{MSE}_{\mathrm{simple}}$ and $\mathrm{MSE}_{\mathrm{DKF}}$ as a function of the process noise N_0 (from left to right: $T_s = 10\,\mathrm{s}, 1\,\mathrm{s}, 0.1\,\mathrm{s}$; $\sigma_{v,1} = \sigma_{v,2} = 1\,\mathrm{m}$)

$\sigma_{v,1} = \sigma_{v,2} = 1\,\mathrm{m}$. However, the sampling period was varied from to $T_s = 0.1\,\mathrm{s}$ to $T_s = 10\,\mathrm{s}$. 200 measurements per simulation and 1000 Monte Carlo runs were used to average the results.

Changing the sampling period T_s merely results in a shift of the corresponding curves. Their shape is not affected. An increase in the sampling period T_s by a factor of 10 can be compensated for by decreasing the power spectral density of the process noise N_0 by a factor of 1000. This can be explained with the accuracy of the position estimate due to the process noise $\mathbf{Q}^{11}$ in (11) being $\frac{1}{3}N_0T_s^3$.

For high values of N_0, all curves approach the variance of the combined measurements $\sigma^2_{v,\mathrm{comb}} = \frac{\sigma^2_{v,1}\sigma^2_{v,2}}{\sigma^2_{v,1}+\sigma^2_{v,2}} = 0.5\,\mathrm{m}^2$. For low values of N_0, they should approach zero as KFs are able to estimate the position arbitrarily precisely if no process noise is present and if a sufficient number of observations is available. Due to calculating the MSEs only on 200 samples including the initialization phase, this is not the case here.

It can be seen that the difference between the respective curves approaches zero for very small and for very large values of N_0. This can be illustrated as follows. For very small values of N_0, the noise term $\mathbf{w}(k)$ in the state equation (8) approaches zero. Thus, there is practically no process noise whose propagation could be responsible for the statistically dependence of the information of the two LKFs.

On the other hand, very large values of N_0 mean an unreliable prediction. Thus, the predicted states $\hat{\mathbf{x}}_i(k|k-1)$, although correlated, carry almost no information about the current state $\mathbf{x}(k)$. Accordingly, they are given almost no weight compared with the measurements $\mathbf{y}_i(k)$ in calculating $\hat{\mathbf{x}}_i(k|k)$ in the LKFs. Note that the Kalman filters are of little use in this case.

Fig. 3 displays the relative difference

$$\Delta_1 = \frac{\mathrm{MSE}_{\mathrm{simple}} - \mathrm{MSE}_{\mathrm{DKF}}}{\mathrm{MSE}_{\mathrm{DKF}}} \tag{12}$$

between the curves in Fig. 2 as a function of the target maneuvering index [7]

$$\mu = \sqrt{\frac{N_0 T_s^3}{\sigma^2_{v,\mathrm{comb}}}}\,. \tag{13}$$

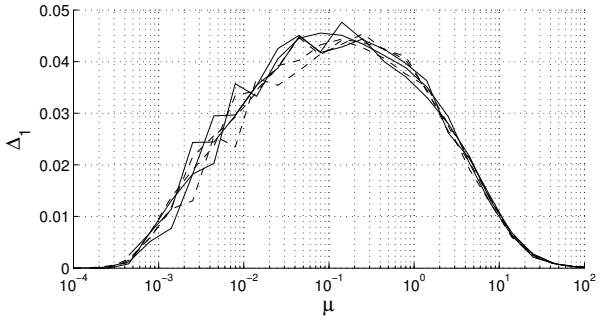

Figure 3: Relative difference between $\mathrm{MSE}_{\mathrm{simple}}$ and $\mathrm{MSE}_{\mathrm{DKF}}$ as a function of the target maneuvering index μ

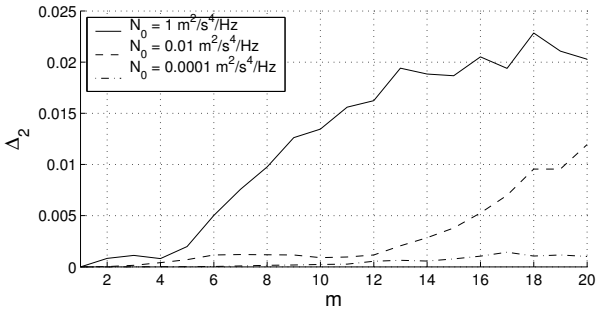

Figure 4: Relative difference between $\mathrm{MSE}_{\mathrm{DKFm}}$ and $\mathrm{MSE}_{\mathrm{DKF}}$ as a function of the the update rate m ($T_s = 1\,\mathrm{s}$, $\sigma_{v,1} = \sigma_{v,2} = 1\,\mathrm{m}$)

The invariance of the curves with respect to μ can be seen clearly. μ is proportional to the ratio between the standard deviation of the position estimate due to the process noise $\sqrt{\mathbf{Q}^{11}}$ and the measurement noise $\sigma_{v,\mathrm{comb}}$. Thus, it can serve as an indicator for how much weight is given to the predicted estimate and the measurements during the fusion process, respectively. The dotted curves demonstrate that the same is true for a constant sampling period $T_s = 1\,\mathrm{s}$ and varying measurement noises $\sigma_{v,1} = \sigma_{v,2} = 0.1\,\mathrm{m}$ to $10\,\mathrm{m}$.

The maximum of the curves in Fig. 3 is rather broad. It ranges approximately from $\mu = 5 \cdot 10^{-3}$ to $\mu = 5$. Thus, many typical scenarios for applying Kalman filters fall within this range. Note that in Fig. 3 the variance of the estimated difference becomes bigger for smaller values of the target maneuvering index μ. This is due to the errors of the state estimate of a KF becoming more correlated in time for such values of μ, thus, reducing the effective number of samples on which the average in (12) is performed.

It remains to be examined how quickly the maximal degradation of 4 to 5 % as indicated in Fig. 3 is reached. To this end, Fig. 4 shows the relative difference

$$\Delta_2 = \frac{\mathrm{MSE}_{\mathrm{DKFm}} - \mathrm{MSE}_{\mathrm{DKF}}}{\mathrm{MSE}_{\mathrm{DKF}}} \tag{14}$$

between the MSE of the position component in $\hat{\mathbf{x}}_{\mathrm{DKFm}}(k|k)$ and $\hat{\mathbf{x}}_{\mathrm{DKF}}(k|k)$ as a function of the update rate m for three interesting values of N_0. Again, the sampling period was set to $T_s = 1\,\mathrm{s}$ and the measurement noises to $\sigma_{v,1} = \sigma_{v,2} = 1\,\mathrm{m}$. This time 10000 Monte Carlo runs were performed on simu-

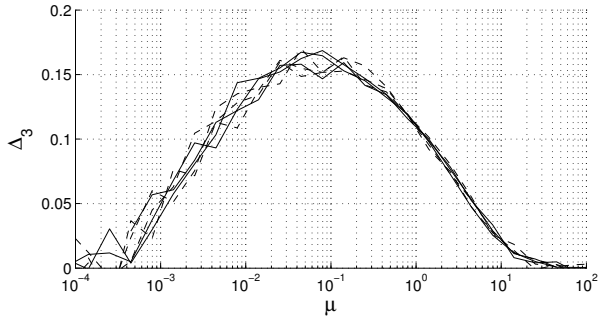

Figure 5: Relative difference between true and estimated MSE of $\mathrm{DKF}_{\mathrm{simple}}$ as a function of the target maneuvering index μ

lations with 200 measurements.

It can be seen that the difference increases more slowly for smaller spectral densities of the process noise N_0. This can be explained with the state vector $\mathbf{x}(k)$ changing only slowly in these scenarios. Therefore, the estimate of the terms correcting for the correlation between $\hat{\mathbf{x}}_1(k|k)$ and $\hat{\mathbf{x}}_2(k|k)$ of the DKFm stay longer an accurate estimate of the correct terms.

As a result, it can be concluded that for all simulated scenarios the communication rate between the LKFs and the FC can be reduced by at least a factor of 8 without introducing an additional error of more than 1 %. Furthermore, for sensors producing measurements at a high frequency, i.e. a scenario where a reduction in communication rate is likely to be desirable, the error due to infrequent communication is typically even smaller due to the short sampling period T_s and, thus, the small target maneuvering index μ.

KFs do not only produce state estimates $\hat{\mathbf{x}}$ but also calculate an accuracy of these estimates in form of the error covariance matrix $\mathbf{P}$. As stated earlier, the DKF estimates its accuracy correctly whereas the $\mathrm{DKF}_{\mathrm{simple}}$, although performing slightly worse, estimates its accuracy even higher than the one of the DKF.

Fig. 5 shows this difference Δ_3 between true and estimated MSE of the $\mathrm{DKF}_{\mathrm{simple}}$ as a function of the target maneuvering index μ. The "true" MSEs were thereby averaged on 5000 Monte Carlo runs. The shape of these curves is very similar to the ones in Fig. 3 for the difference between the true MSE of the $\mathrm{DKF}_{\mathrm{simple}}$ and the one of the DKF. The maximum is only higher at around 16 %. This overestimation presents a significant drawback of the $\mathrm{DKF}_{\mathrm{simple}}$ as the correct prediction of the accuracy is a big advantage when designing a system.

4. ASYNCHRONOUS MEASUREMENTS

Equations (3) and (4) do not only require the LKFs to communicate with the FC after each measurement. Synchronous measurements are implicitly assumed, too. On the other hand, the results of the previous section have shown that the error introduced due to infrequent communication is likely to be almost negligible. Thus, a very simple alternative seems viable: The LKFs all run at their own observation rate communicating with the FC only at predetermined times as defined by the sampling period T_{FC}.

To this end, the LKFs must be able to determine predicted state estimates $\hat{\mathbf{x}}_i(t_1|t_2)$ along with the corresponding error covariance matrices $\mathbf{P}_i^{-1}(t_1|t_2)$ for arbitrary times t_1 and t_2 corresponding to multiples of the sampling period of the FC and the LKF, respectively. This requires the matrices $\mathbf{F}$ and $\mathbf{Q}$ to be set up for arbitrary time intervals. As far as $\mathbf{F}$ is concerned and as (1) is normally derived from a continuous model, this task is likely to be trivial.

As far as $\mathbf{Q}$ is concerned, the discrete white noise sequence $\mathbf{w}(k)$ in (1) has to be assumed to be generated from a continuous white noise sequence $u(t)$ as shown for a constant velocity model in (10). The frequently found assumption of $\mathbf{w}(k)$ being produced by a discrete white noise sequence $u(k)$

$$\mathbf{w}_2(k) = \begin{bmatrix} \frac{1}{2}T_s^2 \\ T_s \end{bmatrix} u(k) \tag{15}$$

with variance σ_u^2 cannot be made. This model implicitly assumes $u(k)$ to be constant between two samples. If this assumption is true for a given sampling period T_s, it cannot be true for any other T_s [7].

5. CONCLUSIONS

This paper focused on the impact, infrequent communication will have on the performance of a DKF. As a result it can be concluded that for all simulated scenarios the communication rate between the LKFs and the FC can be reduced by at least a factor of 8 without introducing an additional error of more than 1 %. Based on this finding, a simple approach to deal with asynchronous measurements was presented. On the other hand, the DKF significantly overestimates its accuracy if the correlation between the inputs is not taken into account.

REFERENCES

[1] B.S. Rao and H.F. Durrant-Whyte, "Fully decentralised algorithm for multisensor Kalman filtering," *IEE Proceedings-Control Theory and Applications*, vol. 138, no. 5, pp. 413–420, Sep 1991.

[2] N. Strobel, S. Spors, and R. Rabenstein, "Joint Audio-Video Object Localization and Tracking," *IEEE Signal Processing Magazine*, vol. 18, no. 1, pp. 22–31, 2001.

[3] M.E. Liggins, C.-Y. Chong, I. Kadar, M.G. Alford, V. Vannicola, and S. Thomopoulos, "Distributed Fusion Architectures and Algorithms for Target Tracking," *Proceedings of the IEEE*, vol. 85, no. 1, pp. 95–107, Jan 1997.

[4] K.C. Chang, R.K. Saha, and Y. Bar-Shalom, "On Optimal Track-to-Track Fusion," *IEEE Transactions on Aerospace and Electronic Systems*, vol. 33, no. 4, pp. 1271–1276, Oct 1997.

[5] A.T. Alouani and T.R. Rice, "On optimal asynchronous track fusion," in *First Australian Data Fusion Symposium*, Nov 1996, pp. 147–152.

[6] R.G. Brown, *Introduction to Radom Signal Analysis and Kalman Filtering*, New York: John Wiley & Sons, 1983.

[7] Y. Bar-Shalom and T. Fortmann, *Tracking and Data Association*, New York: Academic Press, 1988.